Determination of Thermal Contact Resistance in Two-Layer Composites by Flash Method

Katsunori INOUE* and Etsuji OHMURA**

Abstract

A new method by the laser flash method for determining the thermal contact resistance at the interlayer surfaces of two-layer composites are proposed. The time required for the temperature to rise 50 percents, for example, of the maximum temperature increase is read from the temperature versus time curve of the rear surface obtained by experiments. These results are used for the numerical computation based on the theoretical equation of the temperature increase of the rear surface and an iteration method, for example, regula falsi. The influence of the error of each parameter, that is, thickness of each layer, measuring time and thermophysical properties on the measured results is investigated. The present method is applied to some joining specimens and the effectiveness of this method is confirmed. Furthermore, temperature dependence of the thermal contact resistance is also investigated.

KEY WORDS: (Thermophysical Properties) (Thermal Contact Resistance) (Two-Layer Composites) (Flash Method)

1. Introduction

In recent years, the application of layer composites, especially joining ceramics with metals or coating materials on substrates, has rapidly increased in many fields. It is becoming important to estimate the bonding strength of layer composites nondestructively. Thus it is an interesting problem to find the thermal contact resistance at the interlayer surfaces of layer composites. In this paper, a new method by the laser flash method for determining the thermal contact resistance of two-layer composites are proposed.

The flash technique[1]-[3] or stepwise heating technique[4] for measuring thermophysical properties of homogeneous materials has been already adapted to layer composites to find the thermophysical properties. But there are very few reports about determining the thermal contact resistance of layer composites by the transient method except for a few examples in Ref. 3), in which Taylor and Lee measured it using the flash method by comparing the temperature versus time curve obtained by experiments and the theoretical curve. Clear procedure to determine the thermal contact resistance isn't shown in their report, and their method will take much time.

In the present method using the laser flash technique, the thermal contact resistance can be determined easily by the numerical computation based on the theoretical equation of the temperature increase of the rear surface and an iteration method; such as regula falsi. In this method, the time required for the temperature to rise 50 percents, for example, of the maximum temperature increase is only read from the temperature versus time curve. The present method is applied to some joining specimens, and the effectiveness of this method is confirmed. Furthermore, temperature dependence of the thermal contact resistance is also investigated.

2. Theory of Measurement

The schematic diagram of the geometry of a two-layer composite is shown in **Fig. 1**. In the flash method, the front surface of the sample is subjected to a short radiant energy pulse and the resulting temperature history of the rear face is recorded. To solve the heat conduction equation with the appropriate boundary conditions and the initial conditions, the following assumptions are made:

(1) one dimensional heat flow,
(2) no heat loss from the sample surfaces,
(3) each layer is homogeneous,
(4) all thermophysical properties of the two layers are known,
(5) thermal contact resistance between layers is uniform,
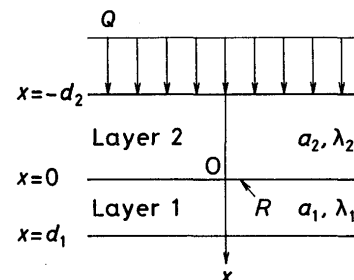(6) heat pulse is uniformly absorbed on the front surface.

Fig. 1 Diagram of two-layer composite.

The heat conduction equation for each layer is mathematically described in the following way:

$$\frac{\partial^2 T_i}{\partial x^2} - \frac{1}{a_i}\frac{\partial T_i}{\partial t} = 0, \quad i = 1, 2 . \tag{1}$$

The boundary conditions are

$$\left[\frac{\partial T_1}{\partial x}\right]_{x=d_1} = 0 , \tag{2}$$

$$\left.\begin{array}{c} \left[\lambda_1\dfrac{\partial T_1}{\partial x} - \lambda_2\dfrac{\partial T_2}{\partial x}\right]_{x=0} = 0 , \\[2ex] \left[\dfrac{\partial T_1}{\partial x} + \dfrac{1}{\lambda_1 R}(T_2 - T_1)\right]_{x=0} = 0 , \end{array}\right\} \tag{3}$$

$$\left[\frac{\partial T_2}{\partial x} + \frac{Q\delta(t)}{\lambda_2}\right]_{x=-d_2} = 0 , \tag{4}$$

and the initial conditions are

$$\left[T_i\right]_{t=0} = 0 , \quad i = 1, 2 \tag{5}$$

where T, a, λ, R and Q are temperature increase, thermal diffusivity, thermal conductivity, thermal contact resistance at the interlayer surfaces and the heat input per unit area on the front surface, respectively. The subscripts 1 and 2 mean the properties of each layer.

By using Laplace transform and inversion formula, the equations (1) to (5) can be solved theoretically, and the normalized temperature of the rear face is represented as Eq. (6)[3].

$$\Theta = 1 + 4\,(\lambda^* d^* + \gamma^2)$$

$$\times \sum_{n=1}^{\infty} \frac{e^{-\beta_n{}^2\gamma^2 t^*}}{\left[\begin{array}{l}(\lambda^*+\gamma)(d^*+\gamma)\cos\beta_n(d^*+\gamma)+(\lambda^*-\gamma)(d^*-\gamma)\cos\beta_n \\ \times(d^*-\gamma)-\gamma\lambda^* R^*\,[\beta_n\,\{(d^*+\gamma)\sin\beta_n(d^*+\gamma) \\ -(d^*-\gamma)\sin\beta_n(d^*-\gamma)\} - \{\cos\beta_n(d^*+\gamma) \\ -\cos\beta_n(d^*-\gamma)\,\}\,] \end{array}\right]} , \tag{6}$$

where

$$\gamma = \sqrt{\frac{a_1}{a_2}} , \quad \lambda^* = \frac{\lambda_1}{\lambda_2} , \quad d^* = \frac{d_1}{d_2} , \quad R^* = \frac{\lambda_2 R}{d_2} ,$$

$$t^* = \frac{a_2 t}{d_2{}^2} , \tag{7}$$

$$\Theta = (1 + \frac{\lambda_1 a_2 d_1}{\lambda_2 a_1 d_2})\,\frac{\lambda_2 d_2}{a_2 Q}\,T_2\,(d_1, t) , \tag{8}$$

and the β_n is the nth positive root of

$$(\lambda^*+\gamma)\sin\beta(d^*+\gamma) + (\lambda^*-\gamma)\sin\beta(d^*-\gamma)$$

$$+ \beta\gamma\lambda^* R^* \left\{\cos\beta(d^*+\gamma)-\cos\beta(d^*-\gamma)\right\} = 0 . \tag{9}$$

Figure 2 shows some examples of normalized temperature versus dimensionless time curves at the rear surface obtained by computing Eq. (6). Temperature rises gradually delayed as the thermal contact resistance becomes large, and these curves don't cross each other. Because R^* is an unknown and t^* is a variable in Eq. (6), we can represent Θ in the following form

$$\Theta = \Theta\,(R^*, t^*) . \tag{10}$$

We introduce a new parameter t_α^* defined by the following equation

$$\Theta\,(R^*, t_\alpha^*) = \alpha , \tag{11}$$

where $0 < \alpha < 1$.

Let the temperature versus time curve of $R^* = 10$ in Fig. 2, for example, be obtained by temperature measurement, then $t_{0.5}^*$ can be read as 11.41 from the figure when α is set at 0.5. When t_α^* is known and R^* is a variable, $\Theta(R^*, t_\alpha^*)$ is a monotone decreasing function as shown in Fig. 3. Therefore, R^* can be easily determined by solving Eq. (11) through the numerical computation; such as the method of bisection algorithm or regula falsi. In this paper, regula falsi was addopted for the numerical computation and carried out on a mini-computer, HITAC
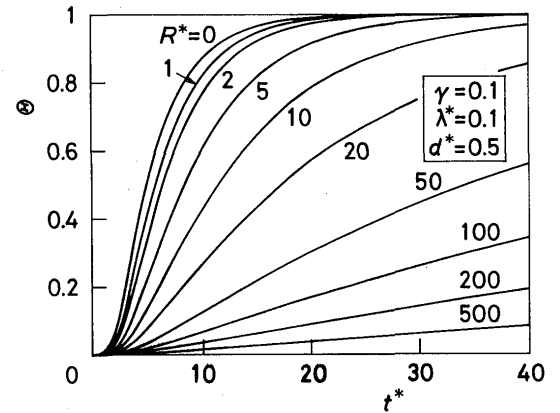
Fig. 2   Normalized temperature versus dimensionless time curves at the rear surface.
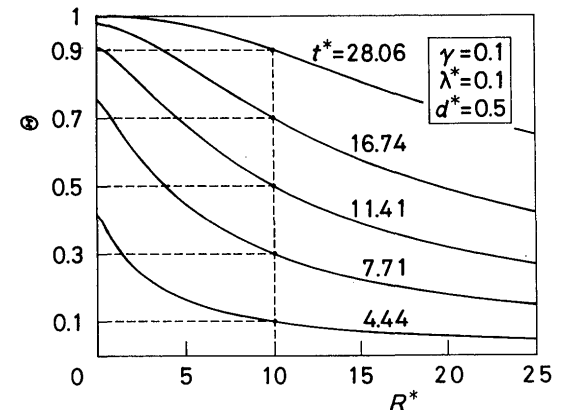
Fig. 3   Function Θ versus R^* for a given time t^*.

E-800. The iteration was stopped when Θ satisfied the following condition for the latest value of R^*.

$$|\Theta| < 0.25 \times 10^{-4} . \tag{12}$$

For many numerical examples, the solutions were obtained within one second at most, and the iteration time was less than ten times, almost.

3. Theoretical Estimation on Accuracy

Since the present method is an indirect measurement method, it is important to investigate the influence of the error of each parameter, that is, thickness of each layer, measuring time and thermophysical properties on the measured results. If the values used for computation, which are denoted by the superscript "′", have relative errors ϵ for the true values d_1, d_2, λ_1, λ_2, a_1, a_2 and $t_{0.5}$, we can express these parameters as

$$\left.\begin{aligned} d_i' &= (1 + \epsilon_{d_i})d_i , \qquad i = 1, 2 \\ \lambda_j' &= (1 + \epsilon_{\lambda_j})\lambda_j , \qquad j = 1, 2 \\ a_k' &= (1 + \epsilon_{a_k})a_k , \qquad k = 1, 2 \\ t_{0.5}' &= (1 + \epsilon_{t_{0.5}})t_{0.5} . \end{aligned}\right\} \tag{13}$$

Substituting Eq. (13) into Eq. (7), the dimensionless value of these parameters can be written as

$$\lambda^{*\prime} = \frac{1 + \epsilon_{\lambda_1}}{1 + \epsilon_{\lambda_2}} \lambda^* ,$$

$$d^{*\prime} = \frac{1 + \epsilon_{d_1}}{1 + \epsilon_{d_2}} d^* ,$$

$$\gamma' = \sqrt{\frac{1 + \epsilon_{a_1}}{1 + \epsilon_{a_2}}} \gamma , \tag{14}$$

$$t_{0.5}^{*\prime} = \frac{(1 + \epsilon_{a_2})(1 + \epsilon_{t_{0.5}})}{(1 + \epsilon_{d_2})^2} t_{0.5}^* .$$

The value of R^* obtained through the present measuring method using the above values has relative error ϵ_{R*}, and it is written as follows:

$$R^{*\prime} = (1 + \epsilon_{R*})R^* . \tag{15}$$

Therefore, R' is expressed by

$$R' = \frac{(1 + \epsilon_{d_2})(1 + \epsilon_{R*})}{1 + \epsilon_{\lambda_2}} R \tag{16}$$

from Eq. (8), and the relative error of R' can be estimated by

$$\epsilon_R = \frac{(1 + \epsilon_{d_2})(1 + \epsilon_{R*})}{1 + \epsilon_{\lambda_2}} - 1 , \tag{17}$$
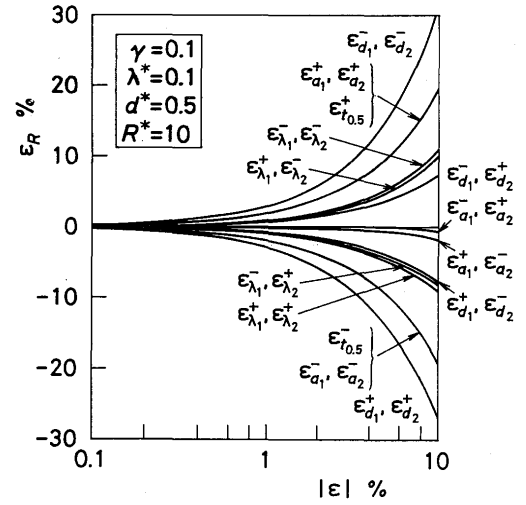

Fig. 4 Influence of each relative error of d_i, λ_j, a_i (i = 1, 2) and $t_{0.5}$ on accuracy of R obtained.

after all.

The estimated results of errors are shown in **Fig. 4** for the same numerical example as the previous section. The abscissa means the absolute values of the relative errors in Eq. (13), and the influence of each error of these parameters on ϵ_R is shown in this figure. ϵ^+ and ϵ^- mean that the error of each parameter is positive and negative, respectively, and the absolute values are equal, when other parameters have no error. It is clear that ϵ_R increases as each relative error increases. When ϵ_{d_1} and ϵ_{d_2} have same sign, the measured error becomes largest, and the errors of time, i.e., $\epsilon_{t_{0.5}}$ and thermal diffusivity are followed. The errors of λ_1 and λ_2 don't affect the final accuracy so much.

4. Experiments and Results

The experiments were carried out with a flash type thermal constant analyzer, TC3000HNC, developed by Sinku-Riko Inc. The apparatus consists of a ruby laser, vacuum system with sample holder and heater, temperature detectors and a data acquisition system. The pulse width of the laser is about 0.7 ms. The temperature detector used was a radiation thermometer (InSb sensor) and the temperature history on the rear surface of the sample was recorded by a transient memory and a pen recorder. The time required for the temperature to rise 50 percents of the maximum temperature increase was read from the temperature versus time curve.

We used four kinds of materials, that is, pure copper (99.99% fine), carbon steel for machine structural use, S45C and tool steel, SK5 and stainless steel, SUS 304 which are equivalent to AISI 1045, ASTM W1-8 and AISI 304, respectively. The thermal diffusivity and conductivity of these materials are shown in **Table 1**. The

Table 1 Thermal diffusivity and conductivity of
materials used.

Sample	a m^2/s	λ W/(m·K)
Cu	1.41×10^{-4}	340
S45C	1.10×10^{-5}	38.2
SK5	1.06×10^{-5}	38.9
SUS 304	3.55×10^{-6}	13.1

recomended values in the references 5) and 6) are used for
the thermophysical properties of Cu, and the thermo-
physical properties of other materials, which will be
influenced by the contents, were measured by the same
apparatus using conventional half-time method of the
laser flash technique for a homogeneous layer. The shape
of the samples was a disk of diameter 10 mm and thick-
ness from 0.7 to 0.8 mm. Both plane surfaces of the disk
were finished finely by a lathe in order to get parallel
planes. Spot welding, resistance brazing and linking by
silicon grease, which we call silicon linking, were used for
joining two-layers.

An example of the recorded temperature history on
the rear surface for a spot-welded composite of SUS 304
stainless steel is shown in **Fig. 5**. This chart was obtained
when the experiment was carried out at the temperature
atmosphere of 771 K in vacuum.

Table 2 shows the half time measured and the thermal
contact resistance at the interlayer surface obtained by
the present method. The thermal contact resistance ob-
tained are seemed to be reasonable in comparison with the
results by Taylor and Lee[3] which are obtained for the
two-layer samples joined by soldering, which are about
3×10^{-5} m^{2}K/W. From this table, it is seen that the
thermal contact resistance for spot welding and resistance
brazing in the present experiments is almost from 3×10^{-6}
to 3×10^{-5} m^{2}K/W, and for silicon linking is about
1×10^{-4} m^{2}K/W.
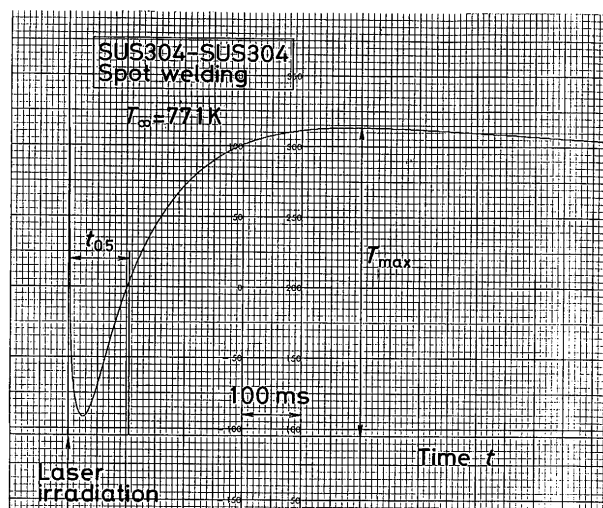
Fig. 5 An example of the recorded temper-
ature history on the rear surface.
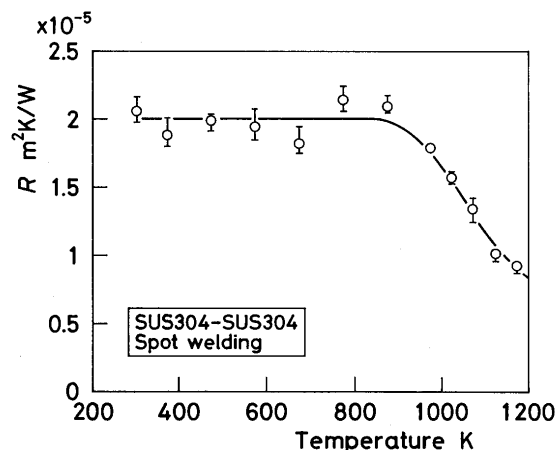
Fig. 6 Temperature dependence of the thermal con-
tact resistance for a spot-welded composite of
SUS 304 stainless steel.

The temperature dependence of the thermal contact
resistance was also examined by the present method for a
spot-welded composite of SUS 304 stainless steel. This

Table 2 The measured half time and the thermal contact resistance obtained
for some two-layer composites.

| Joint method	Layer 1	Layer 2	d_1 mm	d_2 mm	$t_{0.5}$ ms	R m^{2}K/W
Spot welding	S45C	SUS 304	0.767	0.768	62.0	2.32×10^{-6}
	SK5	SUS 304	0.810	0.767	75.5	1.19×10^{-5}
	SUS 304	SUS 304	0.777	0.777	122.5	2.69×10^{-5}
Resistance brazing	Cu	Cu	0.797	0.817	7.7	7.54×10^{-6}
	Cu	S45C	0.769	0.772	22.2	9.14×10^{-6}
Silicon linking	S45C	S45C	0.781	0.773	138	1.14×10^{-4}
	SK5	S45C	0.783	0.773	162	1.35×10^{-4}
	SUS 304	S45C	0.780	0.773	160	1.00×10^{-4}
	SK5	SK5	0.783	0.781	180	1.31×10^{-4}
	SK5	SUS 304	0.783	0.778	219	1.55×10^{-4}
	SUS 304	SUS 304	0.778	0.780	221	1.25×10^{-4}
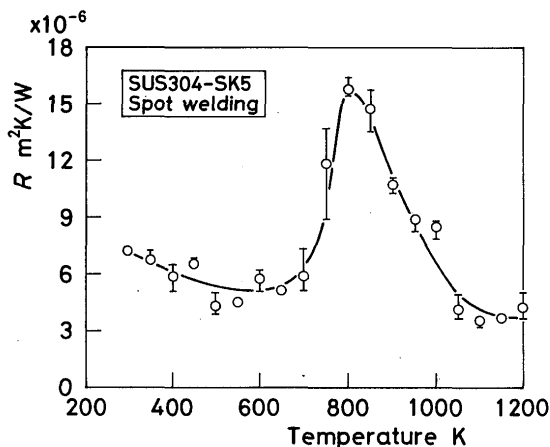
Fig. 7 Temperature dependence of the thermal contact resistance for a spot-welded composite of SUS 304 stainless steel and SK5 too steel.

experiment was carried out in vacuum and the laser pulse was irradiated five times at the same temperature. The results are shown in **Fig. 6**. The circles indicate the mean value of five results obtained at each temperature. The thermal expansion[7] is considered in the computation. The thermal contact resistance doesn't vary so much from the room temperature to about 900K, but it decreases sharply as temperature increases over about 900K. The interpretation of this phenomenon is that the true contact area at the interlayer surface increases rapidly by the volume expansion at the high temperature.

There are two problems that requires consideration for the composites which consist of two different kind layers, that is, the difference of thermal expansion of these layers and the diffusion of elements between the two layers at the high temperature. Strictly speaking, the present measuring method can't be applied to if these problems can't be neglected, but the tendency of the temperature dependence of the thermal contact resistance can be found by using the present method. **Figure 7** shows the temperature dependence of the thermal contact resistance determined by the present method for a spot-welded composite of SUS 304 stainless steel and SK5 tool steel. The thermal contact resistance increases extremely at about 800K. It is interpreted for this remarkable phenomenon that large strain appeared at the weak joining area of interlayer surfaces because of the difference of thermal expansion of the two layers. The thermal contact resistance decreases sharply at higher temperature in Fig. 7 as well as in Fig. 6. The diffusion of elements was confirmed almost uniformly near the interlayer surfaces, by observing the microstructure of the cross section of this specimen with a microscope after the experiment.

5. Conclusion

(1) A new method by the laser flash method for determining the thermal contact resistance at the interlayer surfaces of two-layer composites are proposed. The time required for the temperature to rise 50 percents, for example, of the maximum temperature increase is read from the temperature versus time curve of the rear surface obtained by experiments. These results are used for the numerical computation based on the theoretical equation of the temperature increase of the rear surface and an iteration method, for example, regula falsi.

(2) The influence of the error of each parameter on the measured results was investigated. When the errors of the thickness of each layer have same sign, the measured error becomes largest, and the errors of time, i.e., ϵ_{t_α} and thermal diffusivity are followed. The errors of λ_1 and λ_2 don't affect the final accuracy so much.

(3) The present method was applied to some joining specimens, and it was found that the thermal contact resistance for spot welding and resistance brazing in the present experiments is almost from 3×10^{-6} to $3 \times 10^{-5} \, m^2 K/W$, and for silicon linking is about $1 \times 10^{-4} m^2 K/W$.

(4) Temperature dependence of the thermal contact resistance was also investigated for two spot-welded composites. One consists of only SUS 304 stainless steel, and the other consists of SUS 304 and SK5 tool steel. For the former, it was shown that the thermal contact resistance doesn't vary so much from the room temperature to about 900K, but it decreases sharply as temperature increases over about 900K. For the latter, it was confirmed that the thermal contact resistance increases extremely at about 800K because of the large strain at the interlayer surfaces caused by the difference of thermal expansion of the two layers.

(5) The influence of the uniformity of the bonding strength on the accuracy of the measured results is the subject for a future study.

References

1) Larson, K.B. and Koyama, K., *J. Appl. Phys.*, 39 (1968), 4408.
2) Ang, C.S., Tan, H.S. and Chan, S.L., *ibid.*, 44 (1973), 687.

3) Taylor, R.E. and Lee, H.J., *Rep. 14th Int. Thermal Conductivity Conf.*, (1974), 1.

4) Araki, N. and Natsui, K., *Trans. Japan Soc. Mech. Engrs.*, Ser. B, **49**-441 (1983), 1048. (in Japanese)

5) Touloukian, Y.S., et al., *Thermophysical Properties of Matter, Thermal Conductivity – Metallic Elements and Alloys*, (1973), 68, IFI/Plenum.

6) Touloukian, Y.S., et al., *ibid., Thermal Diffusivity*, (1973), 52, IFI/Plenum.

7) Touloukian, Y.S., et al., *ibid., Thermal Expansion – Metallic Elements and Alloys*, (1975), 1131, IFI/Plenum.